The 7th Annual IEEE International Conference on
Cyber Technology in Automation, Control and Intelligent Systems
July 31-August 4, 2017, Hawaii, USA

A Real-time and Unsupervised Advancement Scheme for Underwater Machine Vision*

Xingyu Chen[1,2], Zhengxing Wu[2], Junzhi Yu[2] and Li Wen[3]

***Abstract*— This paper presents a real-time and unsupervised advancement scheme (RUAS) for underwater machine vision in the natural light condition. RUAS consists of three steps, pre-searching, restoration, and post-enhancing. In pre-searching, we provide a Protected and Greedy Artificial Fish School Algorithm (PGAFSA) to optimize the key parameters of the underwater images, and design an evaluating indicator for the PGAFSA based on the features of underwater images. During the restoration, an image degeneration model is built and the Wiener Filter is employed for noise suppression. Moreover, a filtering-aided color correlation method (FCCM) is then presented against color absorption caused by water. The contrast limited adaptive histogram equalization is employed for the contrast stretch in post-enhancing. Finally, we validated the effectiveness and feasibility of the proposed RUAS with deep-sea environmental videos and practical underwater environments.**

I. Introduction

Underwater vehicle has gradually become an attractive research hotspot. As an excellent underwater mobile platform, it is widely utilized for data collection, underwater monitoring [1] and underwater exploration for search and rescue, e.g., Bluefin 21 was applied in the search for Malaysia Airlines Flight 370 and China's manned submersible Jiaolong dived to 7000 meters in the sea for mine exploration and scientific measurement. To perform tasks successfully, high-quality underwater images for environmental perception are always needed. Unlike terrestrial environments, the underwater environments are more complex and frequently changing which leads to a number of challenges for the adaptability of image processing algorithms.

Recently, many researchers obtained much higher quality of the underwater image with advanced devices, for example, traditional computer vision methods like Gray World [2] and White Patch [3] are used in color correction. Torres-Mendez *et al.* employed a Markov Random Field to represent the relationship between color depleted and color images [4]; Fang *et al.* proposed a single image enhancement approach based on image fusion strategy to enhance the underwater image [5]; Li *et al.* presented a systematic underwater image enhancement method including an underwater image dehazing algorithm and a contrast enhancement algorithm for high-quality underwater images [6]; Iqbal *et al.* provided the Integrated Color Model and Unsupervised Color Correction Method for white balance and contrast stretch [7] [8]. Chiang *et al.* designed a novle algorithm for wavelength compensation and image dehazing to obtain the underwater images with significantly enhanced visibility and superior color fidelity [9]; Hitam *et al.* utilized the Contrast Limit Adaptive Histogram Equalization (CLAHE) to enhance the contrast [10]. Recently, Peng and Cosman proposed a depth and background light estimation method for underwater scenes based on image blurriness and light absorption, which can be used to restore and enhance underwater images [11]. Besides, many studies try to address the issue from the physical level. Typically, Schechner and Karpel employed a polarizer in front of their camera [12]. These methods work well for underwater image processing, but few of them took the degeneration model into account or the proposed models are too complex to work in real time. Moreover, most existing algorithms are lacking in the capability of self-adaption and self-adjustment which are very important for a robot working in a changing and complex underwater environment.

On the other hand, many optimization methods are employed to strengthen the image quality. Artificial Fish School Algorithm (AFSA), which features fast convergence speed and low demand for precise mechanism model, is one of them [13]. However, classical AFSA suffers some issues, such as easy optimum loss. Thus, it is worthwhile improving the algorithm. In addition, an indicator to judge whether the processed image or frame performs well is necessary in image processing. Many existing indicators always have some drawbacks, which limit their applications. For example, some indicators need the original images such as mean square error and peak signal to noise ratio [10]; some depend on what the image shows, such as measure of entropy; and some of them only focus on a particular characteristic, e.g., colorfulness metric only pays attention to the color correction in RGB plane [14] and relative contrast enhancement factor only evaluates the property of contrast [15]. Thus, a synthesized indicator is worthy to be designed.

The main purpose of this paper is to provide a real-time and unsupervised advancement scheme (RUAS) for underwater machine vision in natural light. Generally, the RUAS is mainly comprised of pre-searching, restoration, and post-enhancing. In pre-searching, an improved AFSA

*This work was supported by the National Natural Science Foundation of China (nos. 61633004, 61633020, 61603388, and 61633017), by the Beijing Natural Science Foundation (nos. 4164103 and 4161002), and by the Beijing Advanced Innovation Center for Intelligent Robots and Systems under Grant 2016IRS02.

[1]X. Chen is with the University of Chinese Academy of Sciences, Bejing, 100049, China, chenxingyu2015@ia.ac.cn

[2]X. Chen, Z. Wu, and J. Yu are with the State Key Laboratory of Management and Control for Complex Systems, Institute of Automation, Chinese Academy of Sciences, Beijing, 100190, China, chenxingyu2015@ia.ac.cn, zhengxing.wu@ia.ac.cn, junzhi.yu@ia.ac.cn

[3]L. Wen is with the School of Mechanical Engineering and Automation, Beihang university, Beijing, 100191, China, liwen@buaa.edu.cn

named Protected and Greedy AFSA (PGAFSA) which has a better optimization path and increased convergence speed, is provided to obtain the optimal parameters of degeneration model, filter model, and color correction model automatically. As the target function of PGAFSA, a novel evaluating indicator called gradient-referenced histogram-distribution characteristics (GHC) is built to synthesize the factors of the color correction, contrast, and haze degree. Since the aquatic robot would not switch its working scene frequently, the parameters can be shared with the following frames after the optimal solution is obtained. If the robot fails to perform its main task (e.g., object detection) continuously, pre-searching can be carried out again. In restoration, Wiener Filter is employed for noise suppression and a filtering-aided color correlation method (FCCM) is also presented against color absorption caused by water. Finally, the post-enhancing course takes charge of contrast stretch with CLAHE.

The remainder of the paper is organized as follows. The underwater image degeneration model, filter model, and FCCM are overviewed in Section II. The PGAFSA and GHC are detailed in Section III. Experimental results are described in Section IV. Finally, Section V concludes the paper and describes an outline of future work.

II. Degeneration Model, Filtering and Color Correction

In this section, we will firstly introduce the restoration part of the RUAS, which plays an fundamental role in the whole image processing. The restoration contains two main processes: deconvolution and color correction, which can be noticed in the flowchart of the RUAS, as shown in Fig. 1.

A. Underwater Image Formation

The light signals are degenerated because of absorption, forward scattering and backward scattering [9] [12], which can be formulated as

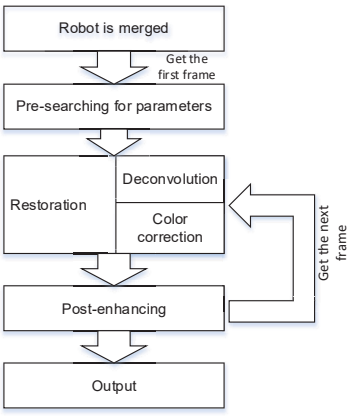

Fig. 1. The flowchart of RUAS

$$v_{\lambda}^{deg} = m(h^{fs}(z), h^{bs}(D,z)) * e^{-\alpha(\lambda,D)z} v_{\lambda}^{orig} + n(D,z) \tag{1}$$

where $e^{-\alpha(\lambda,D)z}$ is the impact of absorption. h^{fs} and h^{bs} are hazing convolution templates caused by forward or backward scatting, and m synthesizes them. n denotes noise cased by backward scatting, while v stands for the original and degraded optical signal.

B. Implementation of Winer Filter with Turbulent Media Model

Hufnagel and Stanley established a general image degeneration model in turbulent media [16], which is expressed in frequency domain as follows

$$\mathcal{H}(u,v) = e^{-k(u^2+v^2)^{5/6}} \tag{2}$$

where k is associated with the intensity of turbulent media.

Considering the consistent effect, we adopt an integrate form $h^{syn}(D,z)$ to replace the term $m(h^{fs}(z), h^{bs}(D,z))$ and by means of fourier transform, we can get

$$\mathcal{V}_{\lambda}^{deg} = e^{-\alpha(\lambda,D)z} \mathcal{H}_{\lambda}^{syn} . * \mathcal{V}_{\lambda}^{orig} + \mathcal{N} \tag{3}$$

where $\mathcal{H}^{syn}$ is formalized by (2). The symbol $.*$ means multiplying the corresponding elements. k is parameterized by D and z, which will be paid greater attention for deconvolution.

Wiener Filter is a classical structure for signal processing. Here, we adopt its simplified form expressed as follows,

$$\hat{\mathcal{V}}_{\lambda}^{orig}(u,v) = [\frac{\mathcal{H}^{c}(u,v)}{|\mathcal{H}(u,v)|^2 + R}] \mathcal{V}_{\lambda}^{deg}(u,v) \tag{4}$$

where R is the reciprocal of signal to noise ratio and can be employed to suppress the noise caused by the backward scattering.

The output signal of Wiener Filter has escaped from the forward and backward scatting ideally.

C. Filtering-aided Color Correction Method

There is another significant effect on contrast caused by filtering, which can be used to make color correct.

FCCM gives a normalized version of the output signals from Wiener Filter. The filter shrinks the contrast, which leads to a narrower-shape curve with an increasing filtering intensity. Note that μ_r/μ_b is constant during this process. Furthermore, if the histogram is normalized into $[0, 255]$, the RGB channels will balance, because the operation makes the distributions more uniform. And higher intensity of the filter will lead to a stronger balance trend.

If color correction is dealt with FCCM blindly, some other features would become worse. For instance, the restored image will perform badly on contrast. Despite the better performance on color correction, the restored image loses other important features, namely over filtering. To avoid the issue, the intensity of filter need to be restricted and Gamma correction is employed for red channel as an assistance, which can be expressed by

$$R_{corrected} = R^{\gamma} \tag{5}$$

TABLE I

THE PROCEDURE OF AFSA AND PGAFSA

AFSA	PGAFSA
Init()	**Init()**
while(not convergent):	**while**(not convergent):
for(number of AF):	**for**(number of AF):
switch(evaluate()):	**if**(is optimal individual):
case follow:	$V, T, \delta \times = \beta_V, \beta_T, \beta_\delta$
follow()	swarm()
if(failed):prey()	**if**(failed):
end if	prey()
case swarm:	**if**(failed):stay()
swarm()	**end if**×**2**
if(failed):prey()	**else**:
end if	follow()
case prey:	**if**(failed):
prey()	swarm()
if(failed):wander()	**if**(failed):
end if	prey()
end switch and for	**if**(failed):wander()
update optimum()	**end if**×**4 and for**
end while	update optimum()
	end while

where γ is a correction factor. It will work when the FCCM is restricted by other factors and fails to perform well on color correction.

III. OPTIMIZATION WITH PGAFSA AND GHC

In this section, we will provide an improved AFSA, named PGAFSA, for underwater image optimization and also designed a novel target function based on the features of underwater images.

A. Classical AFSA

Artificial fish school algorithm is an intelligence optimization method, which is inspired by food searching behavior of fish. Compared with other methods like particle swarm optimization, AFSA owns fast convergence speed but poor searching precision, which just means our requirements. In AFSA, X denotes the individual of artificial fish (AF), and the set $\{X_i\}$ represents the fish school. The fitness function $Y = F(X_i)$ means the food concentration at the position of X_i. D_{ij} denotes the distance between two artificial fish X_i and X_j, and the maximum attempt times of preying is denoted by T. Moreover, V, S and δ represent the visual, step, and density coefficient, respectively.

Generally, the AFSA consists of three typical actions, including following, swarming, and preying. Their mathematical expresses are detailed by [17], and the procedure of classical AFSA is shown in the first column of TABLE I.

B. Gradient-Referenced Histogram-Distribution Characteristics

As for the AFSA, an appropriate fitness function as food concentration is very important. Here, we propose a synthesized evaluating indictor denoted by ξ, according to the features of underwater images. The indicator, namely GHC, is comprised of a haze indicator ψ, a contrast indicator σ, and an imbalance indicator μ, which can be formalized as follows,

$$\xi = \frac{\psi\sigma}{1+\mu} \tag{6}$$

The haze indicator ψ is calculated in gray-scale map and has a range from 0 to 1. It mainly describes the degree of haze with gradient and can be expressed by

$$\psi = \frac{1}{Q}\sum_{i=0}^{p}\sum_{j=0}^{q}\sum_{t=0}^{7} Gradient(\mathcal{V}_g(i,j),t)^2 \tag{7}$$

where $p \times q$ are the image size; $\mathcal{V}_g$ represents the gray-scale map; Q is the total number of added terms. The direction of gradients can be formalized as $t \times 45°$. Obviously, ψ increases if the image becomes more clear.

The imbalance indicator μ denotes the degree of color correction and also has a range from 0 to 1. It equates the sum of the absolute difference of the average values of histogram distribution,

$$\mu = |\mu_r - \mu_g| + |\mu_r - \mu_b| + |\mu_g - \mu_b| \tag{8}$$

where μ_λ denotes the average value of histogram curves. μ decrease with the better color correction.

The contrast indicator σ is expressed by standard deviations of histogram distribution in RGB channels, which depicts the image contrast. It should also be restricted to [0, 1] and can be calculated by

$$\sigma = \frac{1}{pq}\sum_{\lambda}\sqrt{\sum_{i=0}^{255}(ht_\lambda(i)\times i - \mu_\lambda)^2} \tag{9}$$

where $ht_\lambda(i)$ stands for the value of histogram curves at i.

Fig. 2 shows the relationship between the GHC and the key parameters of these models. Note that 0 and 150 separately stand for the minimum and the maximum of each parameter

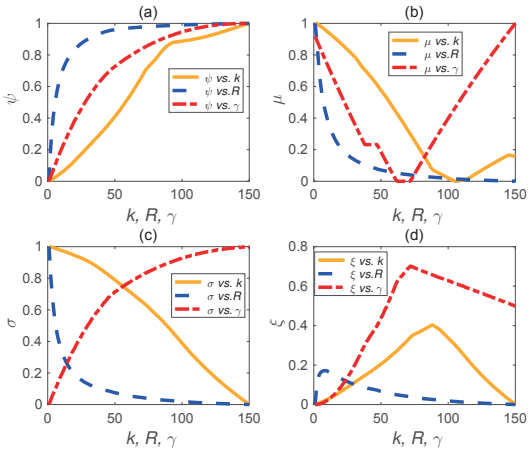

Fig. 2. GHC versus k, R and γ. (a) ψ; (b) μ; (c) σ; (d) ξ.

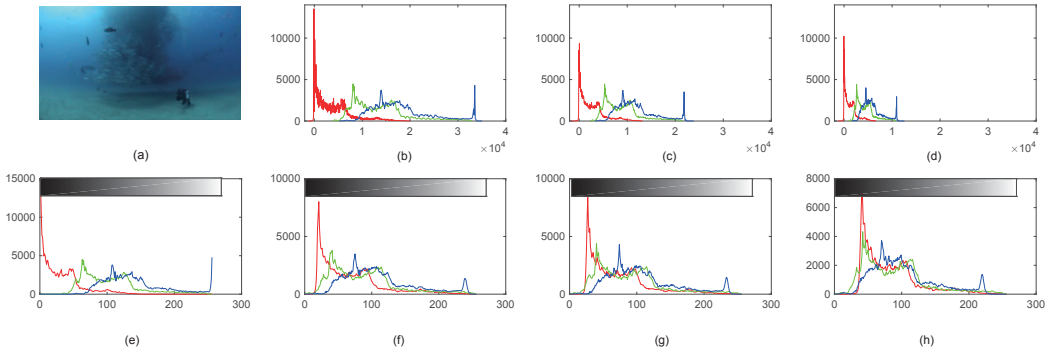

Fig. 3. Underwater image and its histograms. The horizontal axis represents the pixel value of RGB while vertical axis is the statistics of the number of pixels. (a) Underwater image; (e) Original histogram of the image; (b)-(d) Raw histograms of the out put of Wiener Filter with the parameter of (30, 40), (50, 50) and (70, 80); (f)-(h) Normalized histograms of the output of Wiener Filter with the parameter of (30, 40), (50, 50) and (70, 80).

rather than the actual value in models. As for γ, the value 150 represents that Gamma correction is not employed while the value 0 stands for the strongest Gamma correction. ψ tends to increase for higher k, R and γ; σ decreases as k and R increasing, but there is contrary situation versus γ; the trend of μ is not monotonous. As shown in Fig. 2 (d), if fix the other two variables, the peak of GHC can indicate the optimal solution of the interesting parameter.

C. Protected and Greedy Artificial Fish School Algorithm

Firstly, we construct the artificial fish as $X_i = [k, R, \gamma]$ and the food concentration Y_i based on the GHC

$$Y_i = F(X_i) = \frac{\psi\sigma}{1+\mu}\gamma^{0.1} \tag{10}$$

where the term $\gamma^{0.1}$ is employed to prevent X_i from excessive Gamma correction. That is, X_i should correct color with FCCM as much as possible.

Considering that a worse position would be caused by the random action of artificial fish in preying, we provide several effective strategies to solve this issue and also increase the convergence speed.

1) Greedy-following strategy: As for the suboptimal artificial fish, the best behavior is to follow a better one. This is the greed-following strategy. If it fails, it will try to swarm. This strategy will make the algorithm faster and save the time cost of behavior evaluating.

2) Greedy-preying strategy: The optimal artificial fish is deemed that it should has a better density coefficient δ, visual V and maximum attempt times T to provide more chance to prey. Compared with a random step, the greedy-preying strategy will make the artificial fish obtain a better solution directly in preying. Meanwhile, the convergence speed will be enhanced and the optimum solution will not be lost in preying. Mathematically, the optimum is monotonically unabated.

3) Optimum-protection strategy: In classical AFSA, an artificial fish will wander if it fails to follow, swarm and prey. It is pronounced that wandering would possibly lead to optimum loss for the best individual. Therefore, we proposed another behavior for the best AF, namely staying, i.e., holding its solution.

Meanwhile, the small distance of AF is prohibited during the course of initialization. The improved algorithmic procedure is shown in the second column of TABLE I.

IV. Experiments and Results

To validate the proposed RUAS, expecially the FCCM and PGAFSA, for underwater images, extensive experiments have been conducted. For convenience, we choose an underwater video from YouTube in deep-sea experiments, and the practical aquatic experiments have been carried out in Qingdao China. Note that the actual ranges of k, R and γ are $[10^{-7}, 1.5\times10^{-4}]$, $[0.01, 15]$ and $[0.4, 1]$, all of which are normalized as $[0.1, 150]$. The time-related data are obtained with $[640 \times 360]$-pixel-size image and Core i7-6700 CPU with the main frequency upto 3.4 GHz.

A. Experiments on FCCM

The first experiment focused on the effect of color correction with FCCM. The experimental results are shown in Fig. 3. Specially, Fig. 3(a) gives one frame of the employed underwater video, and Fig. 3(e) shows its histogram. In experiments, the raw histograms of the filtered signals were compressed gradually along the horizontal axis with the

TABLE II
THE NUMERICAL ANALYSIS FOR FCCM

Figure	R-B	R/B	Std(R)	Std(B)
(e)	-107.73	0.22	29.11	45.19
(b)	-1.4×10^4	0.22	3.8×10^3	6.0×10^3
(c)	-9.2×10^3	0.22	2.5×10^3	3.9×10^3
(d)	-4.6×10^3	0.22	1.3×10^3	2.0×10^3
(f)	-43.53	0.60	45.25	50.47
(g)	-35.83	0.66	43.96	49.17
(h)	-19.71	0.81	40.94	46.18

Note that R (B) denotes the average value of R-channel (B-channel); Std() represents the standard deviation.

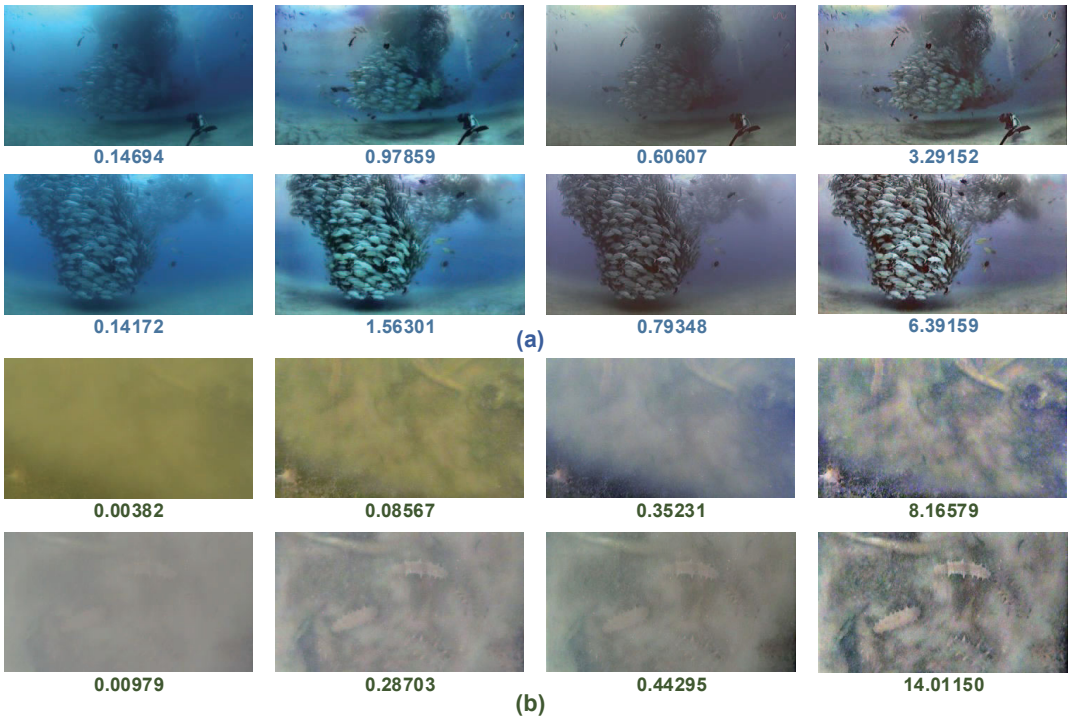

Fig. 5. (a) Experimental results for deep-sea video; (b) Experimental results for practical environment. The first column of (a) and (b) are the original frames; The second are the results of CLAHE; the third are the processed results with filtering and FCCM; and the last column are the eventually results of RUAS. The first row of (a) and (b) is employed as initial frame with PGAFSA and its parameters share with the latter. The data below images are GHC.

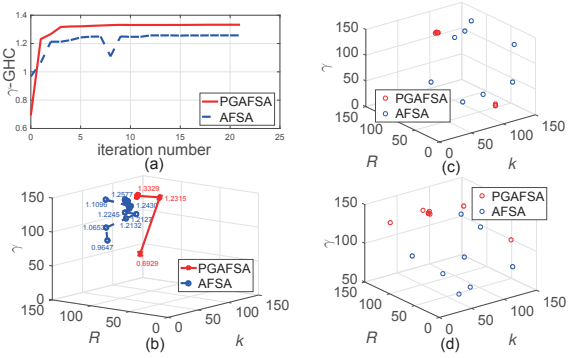

Fig. 4. Comparison results between AFSA and PGAFSA. (a) The convergence curve; (b) Trajectory of optimal individual; (c) The eventual states of AF; (d) The initial state of AF.

increasing filtering intensity, as shown in Fig. 3 (b)–(d). Fig. 3 (f)–(h) give their related normalized data, form which a gradually enhanced trend to color correction can be noticed. The numerical data have been concluded in TABLE II, which is consistent with the theoretical analysis. Thus, FCCM is effective for underwater color correction.

B. Experiments on PGAFSA with GHC

The second experiment focused on the PGAFSA with the indictor GHC. The key parameters in PGAFSA are set as $S = 40$, $V = 60$, $T = 10$, $\delta = 0.2$. The maximum of iterations is 21; the number of AF in AF social is 8 and the size of search space $P \in \Re^3$ is $150 \times 150 \times 150$.

The comparison results between PGAFSA and classical AFSA are shown in Fig. 4. From Fig. 4 (a), we can find that the proposed PGAFSA has a faster convergence and better optimization result even if it has a worse initial state. Besides, the classical AFSA has a optimum loss at the 9th iteration. Finally, the classical AFSA obtains its optimal result with 1.2577 at $[60.6583, 101.549, 139.277]$ after 13 iterations. By contrast, the PGAFSA quickly and monotonically converges to 1.3329 at [60.389; 86.905; 150] after only 7 iterations. Note that each iteration costs 13.52 s in AFSA while only 4.05 s in PGAFSA on the average. Fig. 4 (b) illustrates both optimization trajectories of PGAFSA and classical AFSA, and we can find the PGAFSA obtains a better stability. Moreover, the PGAFSA also perform better for a cluster of AF, as shown in Fig. 4 (c)–(d).

C. Experiments on the Proposed RUAS

The last experiments focused on the proposed RUAS for underwater machine vision. These experiments contained two parts, the first was carried out with a deep-sea video and the second was in a practical underwater environment. In post-enhancing, the CLAHE method was employed. The experimental results are shown in Fig. 5. For convenient, we define (i, j) to indicate the image at the ith row and jth

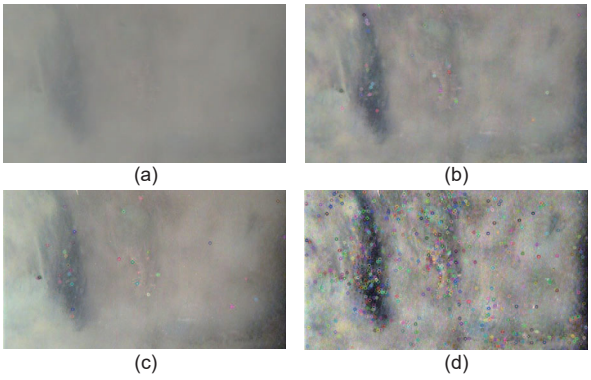

Fig. 6. Test for RUAS with SIFT. (a) The original frame; (b) The CLAHE-processed frame; (c) The filtered frame; (d) The RUAS-processed frame.

column in Fig. 5.

1) Testing RUAS with Deep-sea Environment: We utilized $(1, 1)$ in Fig. 5 (a) as the initial frames. After 8 iterations, about 39.2 s, the optimal solution $[89.9, 17.4, 136.8]$ was obtained. $(1, 3)$ shows the result of filtering as well as FCCM, and proves the prominent effect of FCCM. Through comparing with $(1, 2)$ from the CLAHE only and $(1, 4)$ from the RUAS, we can find the effectiveness of the RUAS on contrast stretch and color correction. The following frames are processed in real time. Among the whole 2217 frames, the maximum processing cost is 49 ms while the minimum is 14.3 ms. It takes 17.5 ms for each frame on average.

2) Testing RUAS in Practical Underwater Environment: Fig. 5 (b) shows the experimental results in a trepang breeding base, Qingdao, China. The 2-m-deep environment is terrible for vision. $(1, 1)$ in Fig. 5 (b) is employed as the initial frame. After 6 iteration, about 28.4 s, the best parameters $[46.4, 107.7, 149.6]$ is obtained by PGAFSA, which performs well for restoration. In order to test the robustness of RUAS, we purposely raised the dust, as shown in $(2, 1)$. In this situation, the RUAS also obtains a good result, as shown in $(2, 4)$. Among the whole 2687 frames, the average time cost for the latter frames is 25.7 ms; the maximum and minimum is 79.1 ms and 15.3 ms, respectively.

SIFT is also employed to test RUAS. As shown in Fig. 6 (a)–(b), SIFT can hardly detect any feature in the original frame, and it is still terrible even though the application of CLAHE. However, aided by RUAS, SIFT can successfully detect rich and salient features, as shown in Fig. 6 (d).

V. Conclusion

In this paper, we have proposed a real-time and unsupervised advancement scheme consisting of pre-searching, restoration and post-enhancing for underwater machine vision. In order to obtain the optimal parameters of restoration model quickly, the PGAFSA is proposed in post-searching. Meanwhile, a novel evaluating indicator, namely GHC, is designed for PGAFSA, based on the features of the underwater images. In restoration, we introduce the classical turbulent media model to describe the degeneration model, and also employe Wiener Filter for deconvolution and restraining noise. A novel and fast color correction method FCCM is also provided. Finally, extensive experiments validate the practicability, validity and robustness of the proposed RUAS and the processing speed can reach about 50 fps.

The future work will focus on the improvement of RUAS and further tasks based on the proposed scheme. The post-enhancing method can be improved and the post-evaluating module is worthy to be involved in RUAS. Furthermore, we intend to grab underwater objects with ROV based on RUAS.

References

[1] D. Shin, S. Y. Na, J. Y. Kim, and S. J. Baek, "Fish robots for water pollution monitoring using ubiquitous sensor networks with sonar localization," In *Proc. 2007 International Conference on Convergence Information Technology*, pages 1298–1303, Nov. 2007.

[2] G. Buchsbaum, "A spatial processor model for object colour perception," *Journal of the Franklin Institute*, 310(1):1–26, 1980.

[3] E. Provenzi, C. Gatta, M. Fierro, and A. Rizzi, "A spatially variant white-patch and gray-world method for color image enhancement driven by local contrast," *IEEE Transactions on Pattern Analysis and Machine Intelligence*, 30(10):1757–1770, 2008.

[4] L. A. Torres-Méndez and G. Dudek, "Color correction of underwater images for aquatic robot inspection," In *Proc. 2005 International Workshop on Energy Minimization Methods in Computer Vision and Pattern Recognition*, pages 60–73, 2005.

[5] S. Fang, R. Deng, Y. Cao, and C. Fang, "Effective single underwater image enhancement by fusion," *Journal of computers*, 8(4):904–911, 2013.

[6] C. Y. Li, J. C. Guo, R. M. Cong, Y. W. Pang, and B. Wang, "Underwater image enhancement by dehazing with minimum information loss and histogram distribution prior," *IEEE Transactions on Image Processing*, 25(12):5664–5677, 2016.

[7] K. Iqbal, R. A. Salam, M. Osman, and A. Z. Talib, "Underwater image enhancement using an integrated colour model," *IAENG International Journal of Computer Science*, 32(2):239–244, 2007.

[8] K. Iqbal, M. Odetayo, A. James, R. A. Salam, and A. Z. Talib, "Enhancing the low quality images using unsupervised colour correction method," In *Proc. 2010 IEEE International Conference on Systems, Man and Cybernetics*, pages 1703–1709, Oct. 2010.

[9] J. Y. Chiang and Y. Chen, "Underwater image enhancement by wavelength compensation and dehazing," *IEEE Transactions on Image Processing*, 21(4):1756–1769, 2012.

[10] M. S. Hitam, E. A. Awalludin, W. N. Jawahir H. W. Yussof, and Z. Bachok, "Mixture contrast limited adaptive histogram equalization for underwater image enhancement," In *Proc. 2013 International Conference on Computer Applications Technology*, pages 1–5, Jan. 2013.

[11] Y. T. Peng and P. C. Cosman, "Underwater image restoration based on image blurriness and light absorption," *IEEE Transactions on Image Processing*, 26(4):1579–1594, 2017.

[12] Y. Y. Schechner and N. Karpel, "Clear underwater vision," In *Proc. 2004 IEEE Computer Society Conference on Computer Vision and Pattern Recognition*, volume 1, pages I–536–I–543, June. 2004.

[13] X. Li, Z. Shao, and J. Qian, "An optimizing method based on autonomous animats: fish-swarm algorithm," *System Engineering Theory and Practice*, 22(11):32–38, 2002.

[14] J. Mukherjee and S. K. Mitra, "Enhancement of color images by scaling the dct coefficients," *IEEE Transactions on Image Processing*, 17(10):1783–1794, 2008.

[15] J. Banerjee, R. Ray, S. R. K. Vadali, S. N. Shome, and S. Nandy, "Real-time underwater image enhancement: An improved approach for imaging with AUV-150," *Sadhana*, 41(2):225–238, 2016.

[16] R. Hufnagel and N. Stanley, "Modulation transfer function associated with image transmission through turbulent media," *Journal of the Optical Society of America*, 54(1):52–60, 1964.

[17] Y. Zhou and H. Huang, "Hybrid artificial fish school algorithm based on mutation operator for solving nonlinear equations," In *Proc. 2009 International Workshop on Intelligent Systems and Applications*, pages 1–5, May. 2009.